Proc. Natl. Sci. Counc. ROC(A)
Vol. 19, No. 2, 1995. pp. 107-112

The Biased Double Phase-Nulling Compensation Scheme for a Fiber-Optic Gyroscope System

JEN-DAU LIN, KUNG-HUNG KUO, AND JENQ-TYNG WU

Institute of Industrial Education
National Changhua University of Education
Changhua, Taiwan, R.O.C.

(Received December 22, 1993; Accepted July 10, 1994)

ABSTRACT

The accuracy of a fiber-optic gyroscope (FOG) system is at its worst state in the straight-fly condition since the rotation signal then is small, and the nonlinear distorsion is serious. However, we can bias two electro-optic modulator with equal amplitude but opposite directions, and use the phase-nulling compensation scheme to lock up the FOG system at its optimal operation point. The improvement in accuracy will be verified both from theoretical principle and experimental results.

Key Words: fiber-optic gyroscope, biased, double-phase-nulling

I. Introduction

Since an airplane (or a missile) may fly straight ahead in the most travelling path, the fiber-optic gyroscope (FOG) system's accuracy at a small rotation rate is very important. However, in this case, the FOG system is just at its worst condition for a small signal/noise ratio and serious nonlinear distorsion.

The problem of an increasing signal/noise ratio can be partly solved by the lock-in amplifier or biasing techniques (Meade, 1982), but the problem of nonlinear distorsion due to small signal level, similar to the crossover distorsion which occurs in a B-type pushpull amplifier, should be solved by using biased compensation (Sedra and Smith, 1987). Thus, we can bias two electro-optic modulators with equal amplitude but opposite directions, and use the phase lock-in techniques to lock up its optimal operation point, thereby improving the accuracy of the FOG System under small rotation rate conditions.

II. Methods

In Fig. 1, the well-known Sagnac phase shift can be represented by the rotation rate Ω as (Arditty and Lefevre, 1981)

$$2\phi_s = \frac{8\pi \cdot A \cdot N \cdot \Omega}{\lambda \cdot c}, \tag{1}$$

where A and N are the loop area and number of circles of the fiber coil, respectively; λ is the optic wavelength; and c is the speed of light.

Referring to Fig. 2, we use a sinewave signal with angular frequency ω_m and amplitude ϕ_m to modulate the light wave with the electrooptic modulator E.O.2. We also use E.O.1 and E.O.2 to generate the compensating phase $\phi_1(t)$ and $\phi_2(t)$ (Page, 1986; Kim and Shaw, 1984; Ebberg and Schiffner, 1985) for the clockwise and counter-clockwise light wave, respectively. Taking into account the Sagnac phase shift, ϕ_s, we can represent the optic electrical fields, E_{cw} and E_{ccw}, one of which is in the clockwise and another in the counter-clockwise direction, as

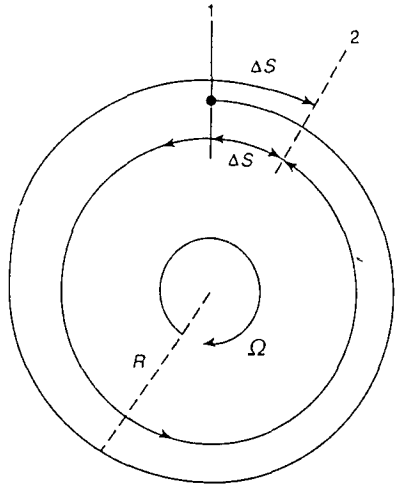

Fig. 1. The Sagnac effect.

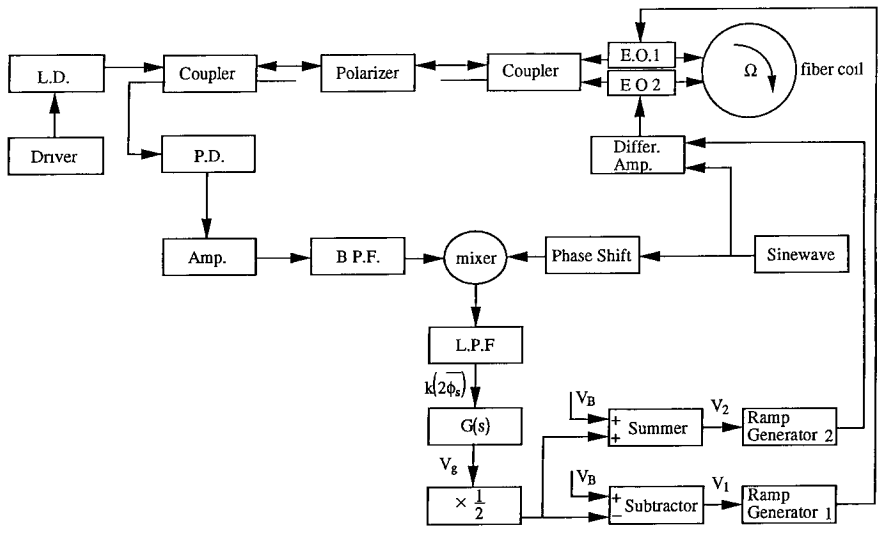

Fig. 2. The schematic figure of the biased double-phase-nulling FOG system.

$$E_{cw}=E_o\exp[j(\omega t+\phi_s+\phi_1(t)+\phi_2(t-\tau) +\phi_m\sin\omega_m(t-\tau))] \quad (2)$$

$$E_{ccw}=E_o\exp[j(\omega t-\phi_s+\phi_1(t-\tau)+\phi_2(t) +\phi_m\sin\omega_m t)], \quad (3)$$

where E_o is the amplitude of the fields; ω is the optic angular frequency; and τ is the time delay of the fiber coil. We obtain an expression I_1 for the light interference signal on the photo detector (P.D.),

$$\begin{aligned} I_1 &= \varepsilon_1\{1+\cos[2\phi_s+(\phi_1(t)-\phi_1(t-\tau))+(\phi_2(t-\tau) -\phi_2(t))+(\phi_m\sin\omega_m(t-\tau)-\phi_m\sin\omega_m(t))]\} \\ &= \varepsilon_1\{1+\cos[2\phi_s+\phi_{\text{compl}}+\phi_{\text{comp2}} -2\phi_m\sin(\frac{\omega_m\tau}{2})\cos\omega_m(t-\frac{\tau}{2})]\} \\ &= \varepsilon_1\{1+\cos[2\phi_s+\phi_{\text{comp}} -2\phi_m\sin(\frac{\omega_m\tau}{2})\cos\omega_m(t-\frac{\tau}{2})]\} \\ &= \varepsilon_1\{1+\cos[2\overline{\phi_s}-\beta\sin(\frac{\omega_m\tau}{2})\cos\omega_m(t-\frac{\tau}{2})]\}, \end{aligned} \quad (4)$$

where ε_1 is a dc term and is proportional to E_o^2; the biased compensation phase, ϕ_{compl} and ϕ_{comp2}, generated from E.O.1 and E.O.2, and some related notations are represented as

$$\phi_{\text{compl}}=\phi_1(t)-\phi_1(t-\tau)>0 \quad (5)$$

$$\phi_{\text{comp2}}=\phi_2(t-\tau)-\phi_2(t)<0 \quad (6)$$

$$\phi_{\text{comp}}=\phi_{\text{compl}}+\phi_{\text{comp2}} \quad (7)$$

$$\overline{2\phi_s}=2\phi_s+\phi_{\text{comp}} \quad (8)$$

$$\beta=2\phi_{\text{m}}. \quad (9)$$

The absolute value of compensation phase, ϕ_{compl} and ϕ_{comp2}, can be represented by the frequency of the ramp waves, i.e. f_1 and f_2, shown in Fig. 3 and Fig. 4, and represented by the input control voltage, V_1 and V_2, of

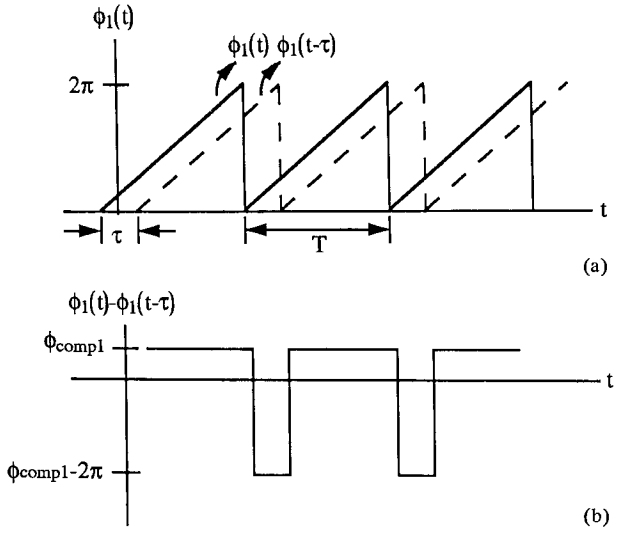

Fig. 3. (a) The phase diagram of $\phi_1(t)$ and $\phi_1(t-\tau)$. (b) The phase diagram of ϕ_{compl}.

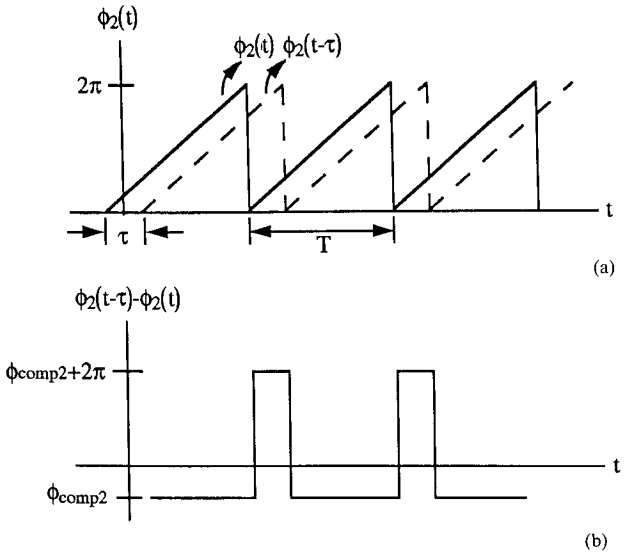

Fig. 4. (a) The phase diagram of $\phi_2(t)$ and $\phi_2(t-\tau)$. (b) The phase diagram of ϕ_{comp2}.

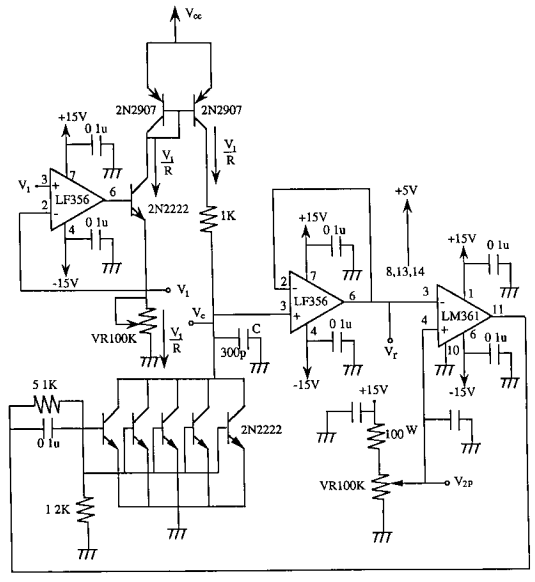

Fig. 5. The circuit of the ramp generator

ramp generators 1 and 2. That is,

$$|\phi_{comp}|_t = 2\pi \cdot \tau \cdot f_i$$

$$= 2\pi \cdot \tau \cdot V_i / (V_{2\pi} \cdot R \cdot C), \quad (10)$$

where $V_{2\pi}$ is the voltage which corresponds to generating a 2π optic phase from the E.O. modulator; R and C are the circuit parameters, the resistor and capacitor of the ramp generator shown in Fig. 5. We design the circuits of the ramp generator, which has a linear relation between the input control voltage and the frequency of the ramp wave as

$$f_i = V_i^f / (V_{2\pi} \cdot R \cdot C). \quad (11)$$

Now we can obtain the relations between ϕ_{comp1} and V_1 or ϕ_{comp2} and V_2, and they is represented in Fig. 6.

To avoid the effect of the high order harmonic term (Bergh *et al.*, 1981), we set

$$\omega_m \tau = \pi. \quad (12)$$

Using Eq. (12), we rewrite Eq. (4) as

$$I_1 = \varepsilon_1 \{1 + \cos(\overline{2\phi_s} - \beta \sin \omega_m t)\}$$

$$= \varepsilon_1 \{1 + \cos\overline{2\phi_s} \cos(\beta \sin \omega_m t)$$

$$+ \sin\overline{2\phi_s} \sin(\beta \sin \omega_m t)\}$$

$$= \varepsilon_1 \{1 + \cos\overline{2\phi_s} [J_o(\beta)$$

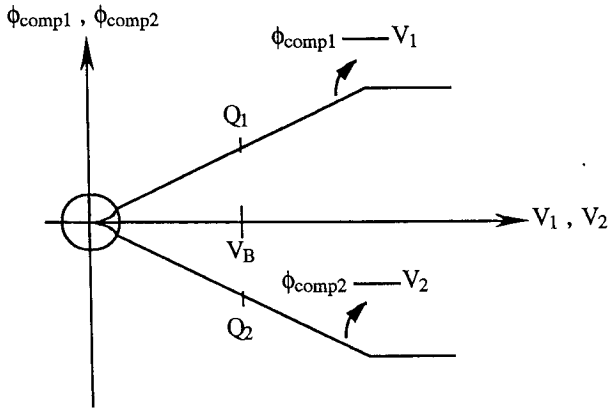

Fig. 6. The mapping diagram of the compensation phase, ϕ_{comp1} and ϕ_{comp2}, and control voltage, V_1, V_2.

$$+ 2 \sum_{n=2,4,\ldots}^{\infty} J_n(\beta) \cos(n \omega_m t)]$$

$$+ \sin\overline{2\phi_s} [2 \sum_{n=1,3,\ldots}^{\infty} J_n(\beta) \sin(n \omega_m t)]\}. \quad (13)$$

Let us filter out the ω_m frequency term from I_1 with a band-pass-filter (B.P.F.); we have

$$I_2 = \varepsilon_2 \{\sin\overline{2\phi_s} \cdot 2 J_1(\beta) \sin \omega_m t\}. \quad (14)$$

Using the well-known lock-in techniques, we mix I_2 signal with $\sin\omega_m t$ first to obtain

$$I_3 = \varepsilon_3 \sin\overline{2\phi_s} \cdot 2 J_1(\beta) \sin^2 \omega_m t$$

$$= \varepsilon_3 \sin 2\overline{\phi_s} \cdot 2J_1(\beta)\left(\frac{1-\cos 2\omega_m t}{2}\right) \quad (15)$$

and put the I_3 signal pass through a low-pass-filter (L.P.F.) to obtain

$$I_4 = \varepsilon_4 J_1(\beta) \sin 2\overline{\phi_s}. \quad (16)$$

If we apply the phase-nulling technique (Cahill and Udd, 1979; Davis, 1981) to make $2\overline{\phi_s} << 1$, then we have $\sin 2\overline{\phi_s} \approx 2\overline{\phi_s}$, and this gives the linear relation between I_4 and $2\overline{\phi_s}$. We will design a feedback compensation control system to meet the $2\overline{\phi_s} << 1$ requirement.

From Fig. 6, the compensation phase, ϕ_{comp1} and ϕ_{comp2}, is not linear with the control voltage, V_1 and V_2, when V_1 or V_2 is very small or very large. The case where V_1 or V_2 is very large will be tolerable for the measurement range and is usually large enough, so we will use it before the nonlinear cases. However, the small rotation rate case where V_1 or V_2 is very small will not be tolerable, and this case will occur frequently in the total travelling path.

The problem of distortion at a small rotation rate state can be solved by shifting the operation point or biasing it with the feedback compensation scheme. We shift the new operation point to Q_1 and Q_2, respectively, as shown in Fig. 6. This can be done by using the following steps: (a) take the output of L.P.F. into $G(s)$ controller; (b) divide the controller's output V_g into two equal parts; (c) add one of these parts with a biased voltage V_B, the midpoint of the linear range, to have voltage V_2; (d) subtract another part from the biased voltage V_B to have voltage V_1; (e) take V_1 and V_2 into E.O.1 and E.O.2 to generate the biased compensation phase, ϕ_{comp1} and ϕ_{comp1}, respectively; the processes discussed here can be referred to in Fig. 2 and Fig. 6. Since the voltage terms V_1 and V_2 can be expressed as

$$V_1 = V_B - \frac{V_g}{2} \quad (17)$$

$$V_2 = V_B + \frac{V_g}{2}, \quad (18)$$

from Eqs. (7) and (10) and Fig. 6, we can have

$$\phi_{comp} = \phi_{comp1} + \phi_{comp2}$$

$$= -2\pi \cdot \tau \cdot V_g / (V_{2\pi} \cdot R \cdot C). \quad (19)$$

Equation (19) has the best linear characteristic because ϕ_{comp1} and ϕ_{comp2} now are biased at their optimal operation point, $V = V_B$; thus, we have solved the nonlinear distorsion for small V_g cases. Also, their dynamic measurement range can be extended to two times greater than before, for two compensators can work at the same time.

III. Results

The simulations were applied to the ramp generator fist. In Fig. 7, the upper channel shows the unbiased control voltage with full-wave rectification wave form, and the lower one shows that the response of the ramp generator is not good at the smallest control voltage which corresponds to a small rotation rate.

If the control voltage was biased with a dc level and had the same waveform shown in Fig. 7, then its smallest control voltage point corresponding to the small rotation rate had good linear response, and the results are shown in Fig. 8.

The system's performance improvement can also be shown directly in the FOG system in Fig. 9 and Fig. 10. The compensation phase, ϕ_{comp}, shown in Fig. 9 deviated from the theoretical prediction for a small rotational signal, but after the bias scheme was applied, it matched the theoretic value very well, and its response is shown in Fig. 10.

IV. Conclusion

A new scheme which uses the biased double-phase-nulling structure to solve the nonlinear distortion problem of a FOG system at a small rotation rate state has been represented here. The biasing techniques can shift the nonlinear distorsion point to some optimal point, and then it is linear in the entire measurement range. The double-phase-nulling struc-

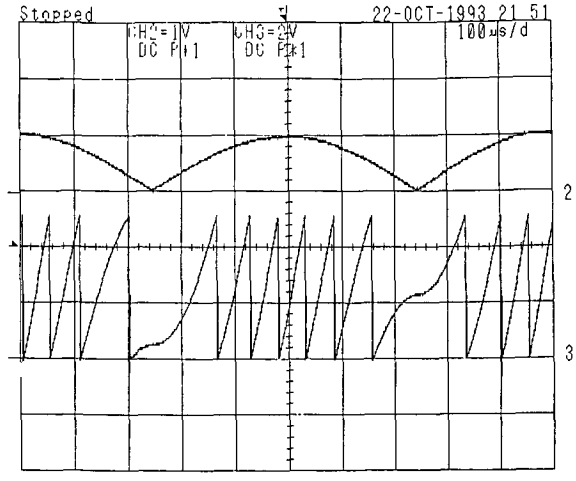

Fig. 7. The nonlinear distortion characteristics. Upper channel: the unbiased control voltage; lower channel: the response of the ramp generator.

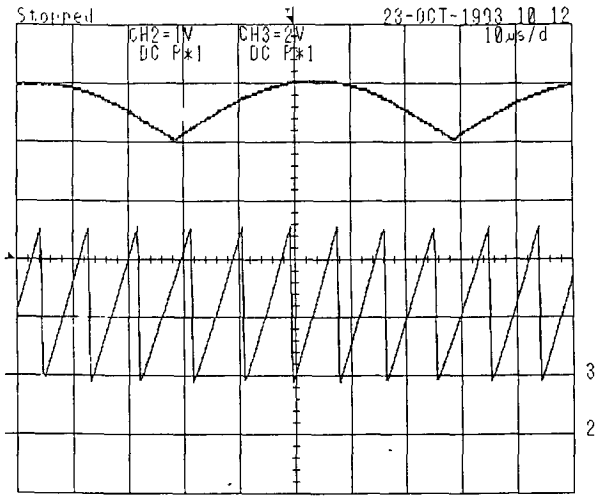

Fig. 8. The cancelling of nonlinear distortion. Upper channel: the biased control voltage; lower channel: the response of the ramp generator.

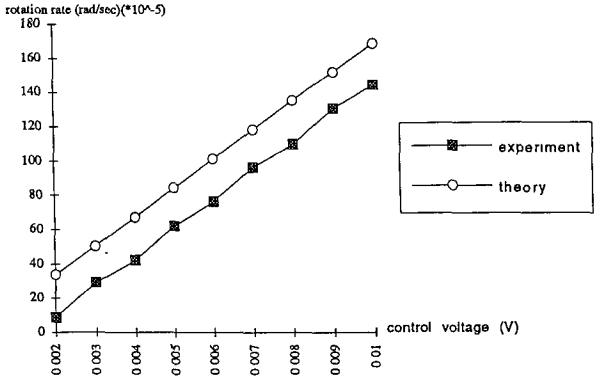

Fig. 9. The comparison between the unbiased system's response and the theoretical response.

ture can eliminate the common path deviation error from the same biasing voltage, V_B, and can be used to increase the dynamic measurement range by two times, for it now has two compensators working at the same time.

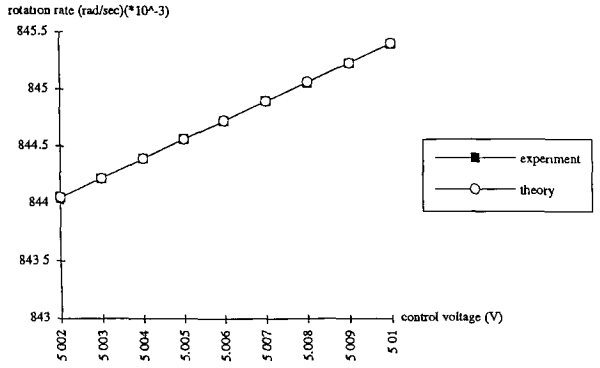

Fig. 10. The comparison between the biased system's response and the theoretical response.

References

Arditty, H. J. and H. C. Lefevre (1981) Theoretical basis for Sagnac effect in fiber gyroscpes. *Springer-Verlag Series in Optical Sciences*, **32**, 44-51.

Bergh, R. A., H. C. Lefevre, and H. J. Shaw (1981) All-single-mode fiber-optic gyroscope with long-term stability. *Opt. Lett.*, **6**, 502-504.

Cahill, R. F. and E. Udd (1979) Phase nulling fiber-optics laser gyro. *Opt. Lett.*, **4**, 93-95.

Davis, J. L. (1981) Closed-loop, low-noise fiber-optic rotation sensor. *Opt. Lett.*, **6**, 505.

Ebberg, A. and G. Schiffner (1985) Closed-loop fiber-optic gyroscope with a sawtooth phase-modulated feedback. *Opt. Lett.*, **10**, 300-302.

Kim, B. Y. and H. J. Shaw (1984) Gated phase-modulation approach to fiber-optic gyroscope with linearized scale factor. *Opt. Lett.*, **9**, 375-377.

Meade, M. L. (1982) Advances in lock-in amplifiers. *J. Phys. E: Sci. Instrum.*, **15**, 395-403.

Page, J. L. (1986) Fiber gyro with electro-optic phase modulation. *Proc. SPIE*, **719**, 53-56.

Sedra, A. S. and K. C. Smith (1987) *Microelectronic Circuits*. 2nd Ed., pp. 555-568. Holt, Rinehart and Winston, New York, NY, U.S.A.

偏壓式雙重相位歸零補償在光纖陀螺儀的應用研究

林正道　　郭坤煌　　吳政庭

彰化師範大學工業教育研究所

摘　要

光纖陀螺儀的精度在導航系統低轉速直飛的狀況下，因訊號微弱及處於非線性失真操作區，而產生精確度的惡化。然而，若以二個電光補償器能對光纖陀螺儀作等強度而反向偏壓的方式，則在歸零鎖相補償下恰能使原惡劣條件，轉成在最佳條件下操作。對於此種精確度的改良方式，文內從學理及實驗二方面去探討發現確有顯著效果。